PHYSICAL REVIEW A VOLUME 60, NUMBER 3 SEPTEMBER 1999

Detailed comparison of above-threshold-ionization spectra from accurate numerical integrations and high-resolution measurements

M. J. Nandor, M. A. Walker, and L. D. Van Woerkom
The Ohio State University, 174 West 18th Avenue, Columbus, Ohio 43210

H. G. Muller
FOM–Institut voor Atoom-en Molekuulfysica, 1098 SJ Amsterdam, The Netherlands

(Received 1 March 1999; revised manuscript received 23 April 1999)

Experimental photoelectron spectra, with high resolution in both kinetic energy and intensity, have been obtained and compared to a high-precision integration of the Schrödinger equation for photoelectron kinetic-energy yields in argon. We find exceptional quantitative agreement between data and calculation over a wide range of kinetic energies and peak laser intensities. In this paper we conclusively show that the single active electron model describes the physics of high-intensity photoionization to a high degree of accuracy. Furthermore, while multiple electrons may be ionized, multielectron effects appear to be completely absent from above-threshold-ionization photoelectron spectra.
[S1050-2947(99)51609-0]

PACS number(s): 32.80.Rm, 34.50.Fa

Multiphoton ionization (MPI) requires a high-intensity laser field to enable electrons to absorb multiple quanta of light in order to ionize; the high intensity also makes absorption of photons in excess of the number needed to ionize [called above-threshold ionization (ATI)] likely [1,2]. With the recent advances in technology, higher and higher order ATI has been achieved, to where noble-gas electrons have presently been seen to absorb upwards of 50–60 photons more than necessary for ionization [3–6].

Many doubly excited states lie within the energy range accessible by such 50-photon absorption. Furthermore, ion spectra clearly show that, as expected, there are double, and even triple, ionizations present at higher intensities in all those species studied [6–8]. We have, then, four mechanisms for ionization: (i) single-electron processes leading to single ionization; (ii) multiple single-electron processes leading to sequential ionization; (iii) multiple-electron excitations leading to single ionization; and (iv) multiple-electron processes leading to multiple ionizations. The pioneering efforts of Shakeshaft and collaborators to fit hydrogen electron spectra obtained by Rottke *et al.* [9] demonstrated that, for small kinetic energies in hydrogen, it was possible to quantitatively compare theory and experiment in this field. Their work, however, was addressing intensities at which only very few ATI orders were present. To date, calculations used to model photoelectron spectra from multielectron atoms still rely on a single active electron (SAE) approximation [5,10–12], which ignores any contributions from either additional electrons or ionizations. For low intensities and low ATI orders these calculations match experimental noble-gas spectra tolerably well. Recent experimental data in xenon [13–16] and argon [17], however, contain highly specific structure in the high-order part of the spectrum, in the area where effects of doubly excited states could be expected. In addition, other features are observed that have no obvious explanation in terms of resonance enhancement by ponderomotively shifting states (Freeman resonances) [18–21], followed by simplified scattering dynamics of a field-driven free electron [22–24]. SAE calculations similar to those discussed in this paper have recently shown [24] that a few of these features in argon photoelectron spectra could be accurately reproduced.

The specific goal of this work was to obtain high-resolution argon photoelectron spectra and compare these to high-precision argon calculations, in order to quantify the single-electron model over a wide range of kinetic energies and laser intensities. Any deviations from the calculations would indicate (i) physics missing from the calculation in the form of temporal coherences, spin-orbit effects, spin-flip collisions in the core, etc., or (ii) physics beyond the single-electron model, such as electron-electron correlations in autoionizing states. Instead, we found that virtually all anomalies, such as various doublet peaks, broad structures, and order-to-order shifts show agreement between experiment and single-electron calculation. We conclude that the vast majority of the physics found in noble-gas, high-intensity photoelectron spectra at 800 nm, over a wide range of kinetic energies and peak laser intensities, can be quantitatively described by a single-electron model. A detailed explanation of the physical mechanisms behind the anomalous features is beyond the scope of this paper, and will be treated elsewhere [25]; however, the remarkable similarities between this SAE calculation and these data clearly imply that multiple-excitation and multiple-ionization processes play little or no part in determining the characteristics of ATI photoelectron spectra in argon.

The experimental setup [16] and numerical methods [24–26] are each discussed elsewhere, but brief descriptions are included here. We use 800-nm 120-fs laser pulses at a 1-kHz repetition rate, focused into an argon-backfilled vacuum chamber, with pressures low enough to assure that there are no space-charge effects. Pulse energy is measured with a power meter and pulsewidth is measured using second-order autocorrelation; using these, the relative intensities between separate data-taking runs are known to within 6.5%. To obtain an absolute intensity, we then match the photoelectron spectra from the intensity at which the 12-photon, $4f$ Freeman resonance appears with the theoretical intensity at

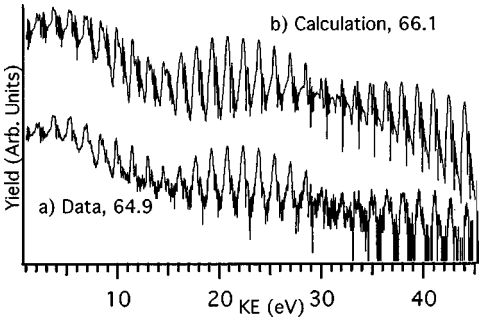

FIG. 1. Sample argon photoelectron spectra for the full range of kinetic energies (plotted on a log scale versus yield) for a certain maximum intensity; intensities are given in TW/cm^2.

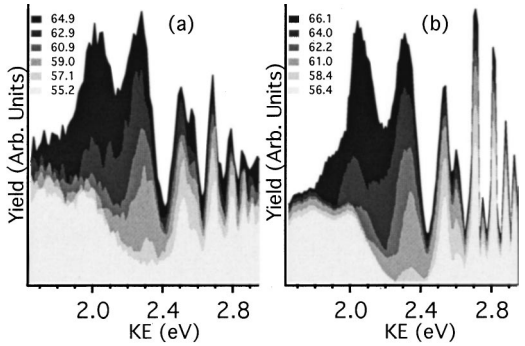

FIG. 2. Sample low-KE spectra for various lower intensities, given in the legend in TW/cm^2. The energy range corresponds to the first ATI order for the given laser parameters. (a) shows experimental data and (b) shows calculations.

which this should occur. We employ a restricted-volume technique [8,27,28] of time-of-flight spectroscopy to determine the kinetic energy (KE) of the electrons. Our electronics allow us a resolution of better than 40 ps and our KE resolution is approximately 20 meV, even for energies greater than 30 eV. The restricted-volume (allowing only photoelectrons ejected from a 500-μm radius surrounding the focus) technique allows for simple spatial deconvolution of the data. A $\lambda/2$ wave plate and polarizing cube combination is used to manipulate the intensity of the light; we obtained photoelectron spectra from 35 different intensities, ranging from 30 to 105 TW/cm^2 and covering a wide range of kinetic energies, which run from 0.4 eV to out past 45 eV.

The calculation is a numerical integration of the Schrödinger equation for a model argon atom in the SAE approximation. The atom is represented by a three-dimensional potential well with a repulsive core, fitted to reproduce the bound-state spectrum of argon. The time-dependent Schrödinger equation is integrated in the velocity gauge, on a radial-position, angular-momentum grid. The propagation uses a half-implicit split-operator scheme accurate to second order in the time step. Fourth-order implicit finite-difference expressions are used to approximate the radial derivatives. A 45-cycle flat-top pulse with a 1/2-cycle turn-on and turn-off essentially results in the atomic continuous wave (cw) response at the corresponding intensity. To account for the spin-orbit splitting of the core, the $J=3/2$ and $J=1/2$ ionization states are each modeled as separate species [29], and then added in a two-to-one (respectively) ratio [30].

The calculations are in the form of the probability of an electron being ejected with a certain KE given a certain *definite intensity*, while the experimental data are in the form of the probability of an electron being ejected with a certain KE given a certain *maximum intensity* of a pulse, given its specific spatial and temporal profile. To convert the calculations into a form similar to the experimental data, two steps were needed. First, the calculated yields were summed over the spatial and temporal profile of the experimental pulse. Essentially, this means that we can compute a signal S, similar to an experimental signal, in terms of the calculated yield for a given intensity $N(I)$, and by performing the double summation

$$S=\sum_{I_i=I_{\min}}^{I_0}\left\{\ln\left(\frac{I_{i+1}}{I_i}\right)\sum_{I_i'=I_{\min}}^{I_i}N(I_i')\left[\sqrt{\ln\left(\frac{I_i}{I_i'}\right)}-\sqrt{\ln\left(\frac{I_i}{I_{i+1}'}\right)}\right]\right\}, \tag{1}$$

where I_0 is the maximum intensity of the pulse. The inner sum is the temporal weighting and the outer sum is the spatial weighting. Spectra from over 550 different integration runs for each core were included in the summation. The various aspects of spatial and temporal summation of the calculated probabilities will be explored in a future publication. The second step in converting the calculations into a form similar to our experimental data is to multiply the calculated probabilities by a transmission function to account for transmission inefficiencies in our instrumentation. The resulting calculated probabilities are now in the form of a spectrum of photoelectron peaks in KE, with each maximum intensity having a different spectrum.

Figures 1–4 each show the results from both the experimental data (a) and the calculations (b). Every trace in the graphs represents a different maximum intensity; the labels on the graphs are given in units of TW/cm^2. The first three figures correspond to one intensity range and the fourth figure corresponds to a higher intensity range; these ranges of intensities are particularly interesting due to the appearance of the 12-photon, $4f$ resonance peak with an increase in intensity for the lower intensities and a growth of the 13-photon-resonant broad structure that appears near the $4d$ Rydberg states. While these data and these calculations are simply small examples of a larger range of intensities and kinetic energies, it should be stressed that the excellent agreement between the experimental data and the calculations is present at all intensities and kinetic energies studied [31].

Figure 1 shows a single maximum intensity from both experiment and calculation for the lower intensity range. Note how the calculation reconstructs the large-scale structure in both magnitude and position. The calculated spectrum has a higher resolution than the experimental spectrum as the kinetic energy increases, and this will be addressed later in this paper. Expanded views of a low-KE region and a high-KE region, but with more intensities shown, are represented by Figs. 2 and 3.

Figure 2 contains the range of kinetic energies corresponding to the first ATI order. Note first how well each individual spectrum in the calculations faithfully reproduces the data. First, the growth of any given peak from intensity to intensity is quite similar between calculation and experiment. Also, the broad feature centered just above 2 eV is mimicked

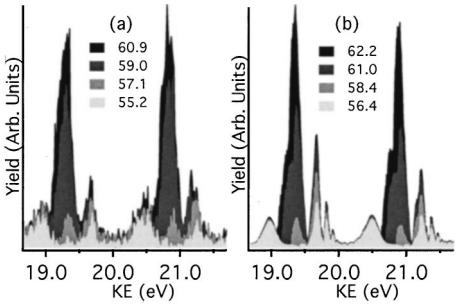

FIG. 3. Sample high-KE spectra for various lower intensities, given in the legend in TW/cm^2. The energy range corresponds to 12th and 13th ATI order for the given laser parameters. (a) shows experimental data and (b) shows calculations.

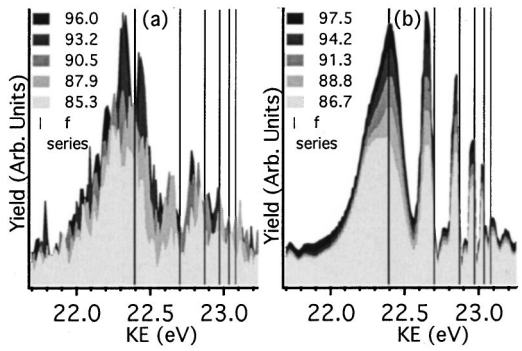

FIG. 4. Sample high-KE spectra for various higher intensities, given in the legend in TW/cm^2. The energy range corresponds to 14th ATI order for the given laser parameters. (a) shows experimental data and (b) shows calculations. The vertical lines show at which energies the resonantly enhanced states (through Rydberg f states) might be expected to appear.

by the calculation extremely well, even though the nature of these states is as yet ambiguous. For states above $n=5$, the calculation produces peaks that are taller and narrower than those found in the experimental data—this is most likely due to the overly large length of time (45 cycles) the calculation uses to ionize the electrons; however, the areas under the peaks are quite similar and so the ionization rates stay faithfully represented.

In addition, the doublet nature of the 12-photon-resonant $5f$ peak (2.55 and 2.60 eV) is well portrayed by the calculations, although there are no Rydberg states located near 2.60 eV [32]. Furthermore, the experimental data show a small shoulder in the $6f$ peak as well, while the calculation shows a small doublet structure for this peak. These structures are present in both the $J=3/2$ and $J=1/2$ calculated spectra separately, so this is not due to differences in spin-orbit cores. It must also be stressed that this phenomenon can also not be due to spin-spin coupling, spin-orbit coupling of the outer electron, temporal coherence, multiple-electron, or multiple-ionization effects, since none of these processes is taken into account in the computation. This leads us to conclude that, while we do not yet understand the mechanisms behind the doublet, we are confident in claiming that the doublet must be due solely to single-electron, single-ionization processes.

Figure 3 contains the range of kinetic energies corresponding to the 12th and 13th ATI orders near the center of the high-order enhancement ''plateau'' at these intensities (see Fig. 1 for a reference). Easily distinguished at the lower intensities are the well-known ''subpeak triplets'' [17,24]. Also, the growth of the peaks is properly reproduced. One discrepancy between the calculations and data is that the calculations display clear structure for states with $n>5$ for high KE, whereas the data do not. The suppression of these resonances in the data could well be due to signal-to-noise problems; given the approximately linear decrease in magnitude from $n=4$ to $n=5$ to $n=6$ in the lower-KE portions of the spectra, one would expect similar decreases in magnitude in the high-KE portions of the spectra; unfortunately, this places the approximate magnitude of the higher KE, $n=6$ peak in the noise and therefore indistinguishable from background. There is also the slight possibility, of course, that some aspect of the physics is missing in the calculation that only manifests itself at higher kinetic energies.

Figure 4 is similar to Fig. 3, but displays results from a higher intensity range. Notice first that the $n>5$ peaks are indeed present (although the data are noisy) in these larger-signal data, which is another indication that the signal-to-noise ratio is the dominant problem in seeing these peaks in the high-KE regions of lower-intensity spectra (see Fig. 3). Also note that, for both experiment and calculation, there is a shift of approximately 50 meV between where these resonances ''should'' appear and where the peaks actually occur. This indicates that, for these higher intensities, the high-KE electrons ionize at a higher resonant intensity than the low-KE electrons. Regardless, since the effect is seen in both data and calculation, this result must also be due to single-electron processes.

In light of the exceptional agreement between experiment and calculation in this paper, the conspicuous absence of multielectron effects in argon photoelectron spectra raises the following question: Given the large density of multielectron states accessible at these intensities, why is there seemingly negligible coupling to the continuum through these channels? If the search for multielectron processes using high fields is to continue, the development of new experimental approaches is vitally important.

On the other hand, thus far argon is the sole noble gas for which extensive, precise calculations have been performed; the chief reason for exploring argon in detail is that, of all the noble gases, it has the clearest high-order enhancement. However, much experimental work has also been done on xenon, which has a larger spin-orbit coupling and autoionizing states that are fairly low lying, needing less than 10 eV to access. It has been shown, for example, that the substructure within the high-order enhancement region [15] is very different between xenon and argon. It is also seen that there are wild ''jets'' and ''wings'' in xenon photoelectron angular distributions [16] that are not correspondingly seen in argon. These issues suggest that extensive, precise calculations for xenon should also be performed.

In conclusion, we have shown that for an extremely wide range of intensities and kinetic energies, it is now possible to model the photoelectron spectra of ultrafast, high-intensity interactions of light and argon atoms, using a model that assumes only single-electron processes. In addition, many ''anomalous'' features that were thought to be due to multiple-electron, multiple-ionization, temporal coherence,

spin-orbit coupling of the outer electron, or spin-spin coupling processes, can now be shown to be completely due to single-electron rescattering dynamics. Electron-correlation theories have been produced over the past few years to explain the anomalous photoelectron spectral features using multielectron and multi-ionization mechanisms [33], and previous data and calculations had not yet been clear enough that it was reasonable to say that these theories could be correct; this work, however, puts to rest the notion that any easily noticeable feature found in the argon ATI photoelectron spectra can come from either multielectron or multiple-ionization mechanisms. The authors themselves find this odd, since it is clear that at least double ionization must be taking place for these intensities, as seen in various ion spectra [34–36]. While a few discrepancies do exist between our calculations and our data, specifically the absence of the $n>5$ resonances in the high ATI orders, which may still be due to such effects, the overwhelming majority of structures and features in the ATI photoelectron spectra of argon can be well modeled by a single-electron calculation, negating the possibility that multiple-excitation or multiple-ionization processes play a significant role in determining the characteristics of these spectra.

The work of M.J.N., M.A.W., and L.D.V.W. is supported by the U.S. Army Research Office under Contract No. DAAG55-97-1-0242. The work of H.G.M. is part of the research program of Fundamental Research on Matter (FOM), which is subsidized by the Netherlands Organization for the Advancement of Science (NWO).

[1] P. Agostini, F. Fabre, G. Mainfray, G. Petite, and N. K. Rahman, Phys. Rev. Lett. **42**, 1127 (1979).
[2] M. Gavrila, *Atoms in Intense Laser Fields* (Academic Press, San Diego, CA, 1992), and references therein.
[3] P. B. Corkum, Phys. Rev. Lett. **71**, 1994 (1993).
[4] G. G. Paulus, W. Becker, W. Nicklich, and H. Walther, J. Phys. B **27**, L703 (1994).
[5] G. G. Paulus, W. Nicklich, H. Xu, P. Lambropoulos, and H. Walther, Phys. Rev. Lett. **72**, 2851 (1994).
[6] L. F. DiMauro and P. Agostini, in *Advances in Atomic, Molecular and Optical Physics* (Academic Press, New York, 1995), Vol. 35, p. 79.
[7] B. Walker, E. Mevel, B. Yang, P. Breger, J. P. Chambaret, A. Antonetti, L. F. DiMauro, and P. Agostini, Phys. Rev. A **48**, R894 (1993).
[8] P. Hansch, M. A. Walker, and L. D. Van Woerkom, Phys. Rev. A **54**, R2559 (1996), although in this experiment we change intensity by adjusting the power, not the position of the focus.
[9] H. Rottke, B. Wolff-Rottke, D. Feldmann, K. H. Welge, M. Dörr, R. M. Potvliege, and R. Shakeshaft, Phys. Rev. A **49**, 4837 (1994).
[10] K. C. Kulander, Phys. Rev. A **38**, 778 (1988).
[11] K. C. Kulander, K. J. Schafer, and J. L. Krause, in *Atoms in Intense Laser Fields*, edited by M. Gavrila (Academic Press, Boston, 1992), p. 247.
[12] G. G. Paulus, W. Nicklich, F. Zacher, P. Lambropoulos, and H. Walther, J. Phys. B **29**, L249 (1996).
[13] K. J. Schafer, B. Yang, L. F. DiMauro, and K. C. Kulander, Phys. Rev. Lett. **70**, 1599 (1993).
[14] G. G. Paulus, F. Zacher, H. Walther, A. Lohr, W. Becker, and M. Kleber, Phys. Rev. Lett. **80**, 484 (1998).
[15] P. Hansch, M. A. Walker, and L. D. Van Woerkom, Phys. Rev. A **55**, R2235 (1997).
[16] M. J. Nandor, M. A. Walker, and L. D. Van Woerkom, J. Phys. B **31**, 4617 (1998).
[17] M. P. Hertlein, P. H. Bucksbaum, and H. G. Muller, J. Phys. B **30**, L197 (1997).
[18] R. R. Freeman, P. H. Bucksbaum, H. Milchberg, S. Darack, D. Schumacher, and M. E. Geusic, Phys. Rev. Lett. **59**, 1092 (1987).
[19] P. Agostini, A. Antonetti, P. Breger, M. Crance, A. Migus, H. G. Muller, and G. Petite, J. Phys. B **22**, 1971 (1989).
[20] R. R. Freeman, P. H. Bucksbaum, W. E. Cooke, G. Gibson, T. J. McIlrath, and L. D. Van Woerkom, in *Atoms in Intense Laser Fields* (Ref. [11]), p. 43.
[21] P. Agostini, P. Breger, A. L'Huillier, H. G. Muller, G. Petite, A. Antonetti, and A. Migus, Phys. Rev. Lett. **63**, 2208 (1989).
[22] B. Yang, K. J. Schafer, B. Walker, K. C. Kulander, P. Agostini, and L. F. DiMauro, Phys. Rev. Lett. **71**, 3770 (1993).
[23] W. Becker, A. Lohr, and M. Kleber, J. Phys. B **27**, L325 (1994).
[24] H. G. Muller and F. C. Kooiman, Phys. Rev. Lett. **81**, 1207 (1998).
[25] H. G. Muller, Phys. Rev. A (to be published).
[26] H. G. Muller, Laser Phys. (to be published).
[27] M. A. Walker, P. Hansch, and L. D. Van Woerkom, Phys. Rev. A **57**, R701 (1998). The kernel for restricted volume is $K=\pi\omega_0^2\Delta z/I$.
[28] R. C. Constantinescu, S. Hunsche, H. B. van Linden van den Heuvell, H. G. Muller, C. LeBlanc, and F. Salin, Phys. Rev. A **58**, 4637 (1998).
[29] The parameters A, B, C, R_x, F, and G as defined in [24] are 5.25, 0.97, 3.7131, 3, 2.0173, and 2.2 for the $P_{3/2}$ state, and 7.3, 1.15, 4.5823, 3.5, 2.380 88, and 1.8 for $P_{1/2}$.
[30] A. L'Huillier, P. Balcou, S. Candel, K. J. Schafer, and K. C. Kulander, Phys. Rev. A **46**, 2778 (1992).
[31] For many more graphs displaying the full range of intensities and kinetic energies, please see our web page at www.physics.ohio-state.edu/~lvw/what/singlee/singlee.html
[32] We plan to further explore the implications of such structures in the future.
[33] P. H. Bucksbaum, A. Sanpera, and M. Lewenstein, J. Phys. B **30**, L843 (1997).
[34] S. Augst, A. Talebpour, S. L. Chin, Y. Beaudoin, and M. Chaker, Phys. Rev. A **52**, R917 (1995).
[35] B. C. Walker, doctoral dissertation, State University of New York at Stony Brook, 1996 (unpublished).
[36] C. Guo, M. Li, J. P. Nibarger, and G. N. Gibson, Phys. Rev. A **58**, R4271 (1998).